The Astrophysical Journal Letters, 958:L3 (6pp), 2023 November 20 https://doi.org/10.3847/2041-8213/ad0239
© 2023. The Author(s). Published by the American Astronomical Society.
OPEN ACCESS

JWST Constraints on the UV Luminosity Density at Cosmic Dawn: Implications for 21 cm Cosmology

Sultan Hassan[1,2,3,21], Christopher C. Lovell[4,5], Piero Madau[6,7], Marc Huertas-Company[8,9,10], Rachel S. Somerville[2], Blakesley Burkhart[2,11], Keri L. Dixon[12,13], Robert Feldmann[14], Tjitske K. Starkenburg[15], John F. Wu[16,17], Christian Kragh Jespersen[18], Joseph D. Gelfand[12,13], and Ankita Bera[19,20]

[1] Center for Cosmology and Particle Physics, Department of Physics, New York University, 726 Broadway, New York, NY 10003, USA; sultan.hassan@nyu.edu
[2] Center for Computational Astrophysics, Flatiron Institute, 162 5th Avenue, New York, NY 10010, USA
[3] Department of Physics & Astronomy, University of the Western Cape, Cape Town 7535, South Africa
[4] Institute of Cosmology and Gravitation, University of Portsmouth, Burnaby Road, Portsmouth PO1 3FX, UK
[5] Astronomy Centre, University of Sussex, Falmer, Brighton BN1 9QH, UK
[6] Department of Astronomy & Astrophysics, University of California, Santa Cruz, CA 95064, USA
[7] Dipartimento di Fisica "G. Occhialini," Università degli Studi di Milano-Bicocca, Piazza della Scienza 3, I-20126 Milano, Italy
[8] Instituto de Astrofísica de Canarias, La Laguna, Tenerife, Spain
[9] Universidad de la Laguna, La Laguna, Tenerife, Spain
[10] Université Paris-Cité, LERMA—Observatoire de Paris, PSL, Paris, France
[11] Department of Physics and Astronomy, Rutgers University, 136 Frelinghuysen Road, Piscataway, NJ 08854, USA
[12] New York University Abu Dhabi, PO Box 129188, Abu Dhabi, UAE
[13] Center for Astrophysics and Space Science (CASS), New York University Abu Dhabi, PO Box 129188, Abu Dhabi, UAE
[14] Institute for Computational Science, University of Zurich, CH-8057 Zurich, Switzerland
[15] Department of Physics & Astronomy and CIERA, Northwestern University, 1800 Sherman Avenue, Evanston, IL 60201, USA
[16] Space Telescope Science Institute, 3700 San Martin Drive, Baltimore, MD 21218, USA
[17] Department of Physics & Astronomy, Johns Hopkins University, 3400 N Charles Street, Baltimore, MD 21218, USA
[18] Department of Astrophysical Sciences, Princeton University, Princeton, NJ 08544, USA
[19] School of Astrophysics, Presidency University, 86/1 College Street, Kolkata 700073, India
[20] Department of Astronomy, University of Maryland, College Park, MD 20742, USA
Received 2023 May 15; revised 2023 October 10; accepted 2023 October 10; published 2023 November 14

Abstract

An unprecedented array of new observational capabilities are starting to yield key constraints on models of the epoch of first light in the Universe. In this Letter we discuss the implications of the UV radiation background at cosmic dawn inferred by recent JWST observations for radio experiments aimed at detecting the redshifted 21 cm hyperfine transition of diffuse neutral hydrogen. Under the basic assumption that the 21 cm signal is activated by the Lyα photon field produced by metal-poor stellar systems, we show that a detection at the low frequencies of the EDGES and SARAS3 experiments may be expected from a simple extrapolation of the declining UV luminosity density inferred at $z \lesssim 14$ from JWST early galaxy data. Accounting for an early radiation excess above the cosmic microwave background suggests a shallower or flat evolution to simultaneously reproduce low- and high-z current UV luminosity density constraints, which cannot be entirely ruled out, given the large uncertainties from cosmic variance and the faint-end slope of the galaxy luminosity function at cosmic dawn. Our findings raise the intriguing possibility that a high star formation efficiency at early times may trigger the onset of intense Lyα emission at redshift $z \lesssim 20$ and produce a cosmic 21 cm absorption signal 200 Myr after the Big Bang.

Unified Astronomy Thesaurus concepts: Cosmology (343); James Webb Space Telescope (2291); Radio interferometers (1345); H I line emission (690); Early universe (435)

1. Introduction

A number of observational facilities are currently or will soon probe the epoch of cosmic dawn ($z > 10$), when the first stars and galaxies are expected to have formed. Results from these facilities are expected to place important constraints on the first astrophysical sources of radiation, including their number density, ionizing emissivity, as well as the physics of their formation.

The James Webb Space Telescope (JWST) is the current flagship space-based infrared observatory, and was specifically designed to probe the epoch of first light as one of the main scientific goals (Robertson 2022). One of the first tantalizing results from early-release JWST data has been the discovery of very high redshift candidate galaxies in NIRCam imaging (e.g., Adams et al. 2023; Bradley et al. 2023; Castellano et al. 2022, 2023; Donnan et al. 2023, 2023; Finkelstein et al. 2022, 2023; Harikane et al. 2022; Naidu et al. 2022b; Atek et al. 2023; Morishita & Stiavelli 2023; Pérez-González et al. 2023; Yan et al. 2023). Not only are these galaxies at much higher redshifts than any galaxy discovered previously by the Hubble Space Telescope (HST), but they are also surprisingly bright. Almost all galaxy formation models struggle to reproduce the number densities of these bright early systems (Finkelstein et al. 2023). Additionally, after performing spectral energy distribution (SED) fitting on the measured fluxes, many authors obtain high stellar masses (Donnan et al. 2023; Harikane et al. 2023b; Labbe et al. 2022) that may be in tension with the astrophysics of early galaxy formation

[21] NASA Hubble Fellow.

Original content from this work may be used under the terms of the Creative Commons Attribution 4.0 licence. Any further distribution of this work must maintain attribution to the author(s) and the title of the work, journal citation and DOI.

(Boylan-Kolchin 2023; Lovell et al. 2023; Kannan et al. 2023; but see McCaffrey et al. 2023; Prada et al. 2023; Yung et al. 2023 for a different interpretation). Given these challenges, it may be important to seek out independent measurements of the source population at very early epochs.

The cosmic microwave background (CMB) spectrum is predicted to show an absorption feature at frequencies below 150 MHz imprinted when the Universe was flooded with Lyα photons emitted from the very first stars and before it was reheated and reionized (Madau et al. 1997; Tozzi et al. 2000). The depth and timing (frequency) of the global 21 cm signal carry a wealth of information about the nature of the first sources and the thermal state of the intergalactic medium (IGM), and can constrain the physics of the very early Universe. The Experiment to Detect the Global EoR Signature (EDGES) team has reported a controversial detection (Bowman et al. 2018) of a flattened absorption profile in the sky-averaged radio spectrum, centered at 78 MHz and with an anomalous amplitude of 0.5 K, placing the birth of the first astrophysical sources at $z \sim 20$.

Such a deep absorption trough implies new exotic physics during cosmic dawn, such as some interaction between dark matter and baryons (see, e.g., Barkana 2018; Muñoz et al. 2018; Slatyer & Wu 2018), or an excess radio background (e.g., Fraser et al. 2018; Pospelov et al. 2018; Feng & Holder 2018; Ewall-Wice et al. 2018; Fialkov & Barkana 2019; Ewall-Wice et al. 2020). It has also been argued (see, e.g., Hills et al. 2018; Bradley et al. 2019; Singh & Subrahmanyan 2019; Sims & Pober 2020) that the EDGES signal may not be of astrophysical origin, and the recent nondetection by the SARAS3 experiment (Singh et al. 2022) confirms earlier concerns.

While both JWST results based on early NIRCam observations in this extreme redshift regime and the nature of a radio absorption signal are highly uncertain, it is of interest to discuss the implications of a bright UV radiation background at cosmic dawn for 21 cm cosmology. In this Letter, we attempt to answer the following question: Can the young galaxies detected by JWST at the highest redshifts provide enough Lyα radiation to mix the hyperfine levels of neutral hydrogen and produce a global 21 cm signal at the redshifts, $z \sim 17$, probed by the EDGES and SARAS3 experiments? We stress that, as in Madau (2018), our analysis focuses on the timing of such a signal and on the constraints imposed by the required Wouthuysen–Field coupling strength on the UV radiation background at first light, and in the presence of different levels of radio background (Feng & Holder 2018; Ewall-Wice et al. 2018). Our analysis does not attempt to explain or dispute the absorption trough claimed by EDGES.

2. UV Luminosity Density at High Redshift

Figure 1 shows estimates of the UV luminosity density, $\rho_{\rm UV}$, from HST (Oesch et al. 2018; Ishigaki et al. 2018; Bouwens et al. 2015), JWST/NIRCam[22] (Donnan et al. 2023; Harikane et al. 2022; Bouwens et al. 2022b), and JWST/NIRSpec (Harikane et al. 2023a), and quoted in the legend for different magnitude faint-end cutoffs of $M_{\rm UV} = -18$ (left panel) and $M_{\rm UV} = -13$ (right panel).[23] All values were obtained by integrating the observed luminosity function (LF) down to the cutoff. Since the faint-end slope α at these early epochs is highly unconstrained, and these measured UV LFs are obtained at fixed α, we assume a level of uncertainty inspired by Bouwens et al. (2022a), where errors in α are shown to evolve from $\sim$1%–2% at $z \sim 2$–3 to $\sim$4%–7% at $z \sim 7$–10. We then conservatively assume a 5% and 10% error in the faint-end slope of the galaxy LF at $z < 10$ and $z > 10$, respectively, and add these uncertainties to JWST data only.

In Figure 1 we also plot the UV luminosity density required to produce a 21 cm feature at $16 < z < 19$ in the "minimal coupling" regime (red box; Madau 2018). This constraint is imposed on the background Lyα flux by the Wouthuysen–Field mechanism that mixes the hyperfine levels of neutral hydrogen and is key to the detectability of a 21 cm radio signal from the epoch of first light (Madau et al. 1997). It yields $\rho_{\rm UV} = 10^{24.52}$–$10^{25}\,(18/(1+z))^{1/2}$erg s^{-1} Mpc^{-3} Hz^{-1} for a proportionality constant ($g = 0.06$) that relates the number density of Lyα photons to the ionizing emissivity (see Equation 10 and associated text in Madau 2018 for more details). In Madau (2018), a fitting function, $\log_{10}(\rho_{\rm UV}/{\rm ergs^{-1}Mpc^{-3}Hz^{-1}}) = (26.30 \pm 0.12) + (-0.130 \pm 0.018)(z-6)$ for a magnitude cutoff $M_{\rm UV} = -13$, was provided to describe a gradual redshift evolution consistent with $4 \leqslant z \leqslant 9$ deep HST observations as well as the minimal coupling 21 cm regime. Since no JWST data were included in Madau's (2018) functional form, we refit for all data including HST, JWST, and the Wouthuysen–Field mechanism (red box). The updated fitting function, $\log_{10}(\rho_{\rm UV}/{\rm ergs^{-1}Mpc^{-3}Hz^{-1}}) = (26.31 \pm 0.16) + (-0.118 \pm 0.019)(z-6)$, and associated 1σ uncertainty are shown in the figure with the red solid line and shaded band.

In addition to the minimal coupling 21 cm regime, we consider the same constraints in the presence of different levels of an additional (beyond the CMB) radio background of brightness temperature $T_{\rm rad}$. Since the brightness temperature of the 21 cm signal scales as

$$\delta T_{21} \propto 1 - \frac{T_{\rm CMB} + T_{\rm rad}}{T_s}, \tag{1}$$

where T_s is the hydrogen spin temperature, the amplitude of the absorption signal can be increased by increasing $T_{\rm rad}$, leading to a multiplicative boost in the canonical absorption signal by the factor $F_{\rm boost} \approx 1 + T_{\rm rad}/T_{\rm CMB}$ in the limit $T_s \ll T_{\rm CMB}$. First, we shall consider a radiation excess by early black hole accretion as proposed by Ewall-Wice et al. (2018), where a boost factor of $F_{\rm boost} \approx 3$ (corresponding to the presence of 1% of the present day black hole mass at $z \sim 17$) was found to reproduce the amplitude of the EDGES detection. This increases the Lyα coupling constraints on $\rho_{\rm UV}$ by the same factor, as shown by the brown box. In this scenario, the best-fit UV luminosity density, $\log_{10}(\rho_{\rm UV}/{\rm ergs^{-1}Mpc^{-3}Hz^{-1}}) = (26.22 \pm 0.15) + (-0.072 \pm 0.017)(z-6)$, has a much shallower redshift evolution. Second, we consider the strong radiation excess detected by the Absolute Radiometer for Cosmology, Astrophysics and Diffuse Emission (ARCADE 2), which is consistent with the CMB at high frequencies and substantially higher than the CMB at low frequencies (Fixsen et al. 2011). Following the fitting function provided by Feng & Holder (2018), we find a boost factor of $F_{\rm boost} \approx 20$, leading to a corresponding increase in the coupling constraint on $\rho_{\rm UV}$ (black

[22] We omit results at $z > 15$ based on a single candidate galaxy that was recently spectroscopically confirmed to be at lower redshift (Naidu et al. 2022a; Zavala et al. 2023; Arrabal Haro et al. 2023).

[23] We extrapolate only down to $M_{\rm UV} = -13$ since most of the reconstructed UV luminosity functions (LFs) from measurements and theory do not show a cutoff at magnitudes brighter than this limit (e.g., see Bouwens et al. 2022a).

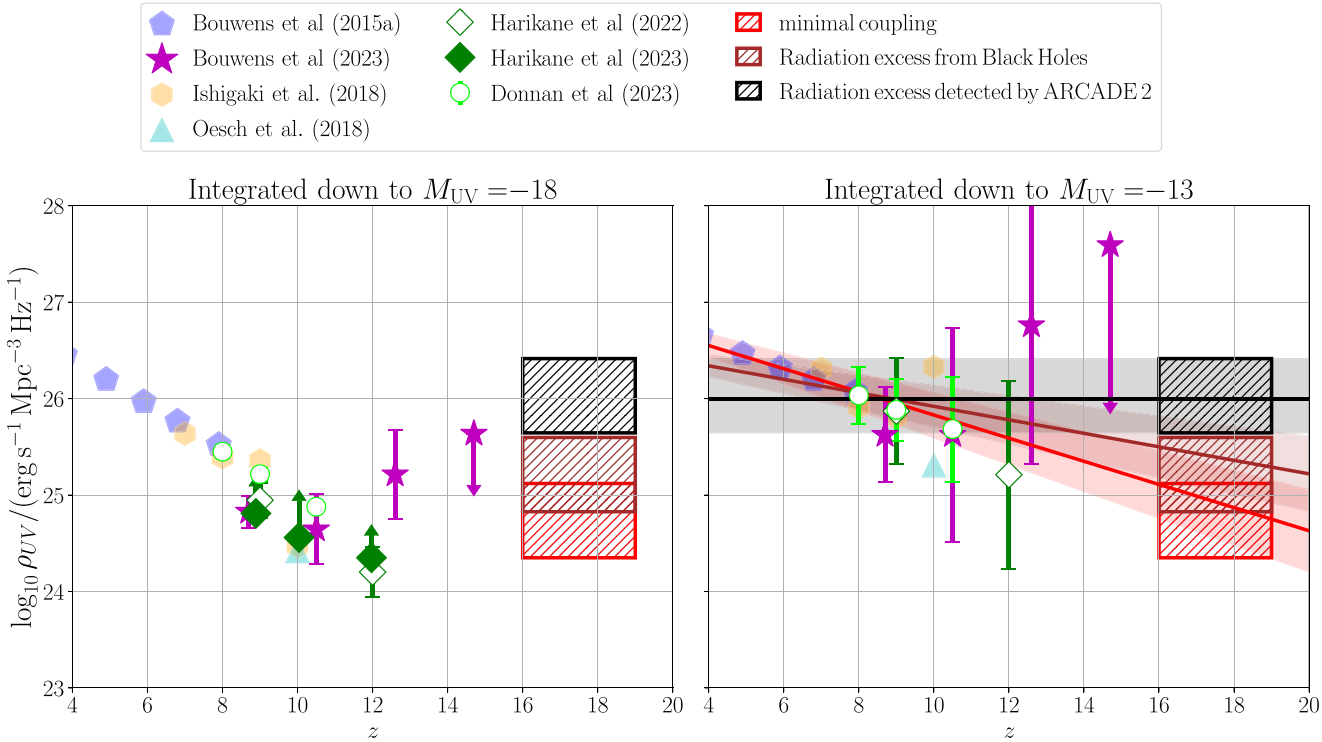

Figure 1. The galaxy UV luminosity density, $\rho_{\rm UV}$, from HST (faint cyan triangles, Oesch et al. 2018; faint orange hexagons, Ishigaki et al. 2018; faint blue pentagons, Bouwens et al. 2015) and JWST (open lime circles, Donnan et al. 2023; open green diamonds, Harikane et al. 2022; magenta stars, Bouwens et al. 2022b), using the measured LF from $z=4$ to $z=14$ for different magnitude cutoffs $M_{\rm UV}=-18$ (left panel) and $M_{\rm UV}=-13$ (right panel). Error bars are added only to JWST data assuming 5% and 10% uncertainties in the faint-end slope at $z<10$ and $z>10$, respectively. The recently confirmed spectroscopic measurements reported by Harikane et al. (2023a) are shown as filled green diamonds. The red box depicts the UV luminosity density needed to produce a 21 cm global signal at $16<z<19$ in the minimal coupling regime (Madau 2018). The brown and black boxes show the enhanced $\rho_{\rm UV}$ required by the presence of a radio background excess produced by early black holes (Ewall-Wice et al. 2018) and following the claimed detection by ARCADE 2 (Feng & Holder 2018), respectively. If JWST LF measurements could be extrapolated down to $M_{\rm UV}=-13$, the ensuing luminosity density would match the gradual redshift evolution predicted by Madau (2018) and the updated fit (red line), providing enough Lyα background radiation to mix the hyperfine levels of neutral hydrogen 200 Myr after the Big Bang. Due to the large uncertainty associated with cosmic variance/faint-end slope of the LF at these early epochs, the enhanced UV luminosity density required by the presence of a radio background excess (brown and black boxes) is also broadly consistent with current JWST and HST data, following shallow (brown line) or flat (black line) evolution in $\rho_{\rm UV}$.

Table 1
Constraints on the Schechter Function Parameter $\phi^\star$ from the UV Luminosity Density Needed to Produce a 21 cm Signal at $z=16$ at Fixed $M^\star_{\rm UV}=-19$ and $\alpha=-2.35$ in the Minimal Coupling Regime and in the Presence of Different Levels of a Radio Background

	$\log_{10}(\rho_{\rm UV}/\rm erg\ s^{-1}\ Mpc^{-3}\ Hz^{-1})$	$\log_{10}\phi^\star$
Minimal 21 cm coupling (Madau 2018)	24.60 ± 0.24	$-4.671^{+0.240}_{-0.246}$
Radiation excess from black holes (Ewall-Wice et al. 2018)	25.24 ± 0.24	$-4.194^{+0.243}_{-0.244}$
Radiation excess by ARCADE 2 (Feng & Holder 2018)	26.06 ± 0.24	$-3.381^{+0.244}_{-0.247}$

box in the figure). This enhanced UV luminosity density is comparable to existing estimates at $z\sim4$–8, and a flat evolution of $\log_{10}(\rho_{\rm UV}/\rm ergs^{-1}Mpc^{-3}Hz^{-1})=26.06\pm0.24$ would reproduce both low- and high-z constraints in this case. This extreme case of a flat evolution in $\rho_{\rm UV}$ is unlikely while the Universe is evolving from $z=20$ to $z=4$. However, we show this extreme case to set an upper limit for the expected shallow redshift evolution in the presence of radiation excess.

Regardless of the magnitude cutoff, we find a general consistency between the early and more recent measurements of the UV luminosity density by HST and JWST. At the limit $M_{\rm UV}=-18$ (left panel in Figure 1), HST and JWST data indicate a rapid decline in $\rho_{\rm UV}$ toward early epochs consistent with the evolving $\rho_{\rm UV}$ expected in constant star formation efficiency models (Harikane et al. 2023a), but inconsistent with the constraints imposed by a possible 21 cm signal centered at redshift $z\sim17$. Extrapolating to fainter magnitudes and integrating down to $M_{\rm UV}=-13$, we find instead that the measurements suggest a milder evolution in $\rho_{\rm UV}$. This suggests that the high-redshift constraints by JWST in the redshift range of $z\sim8$–12 and a 21 cm signal in the minimal coupling regime at $z\sim17$ may all be consistent with an extrapolation of the declining galaxy UV luminosity density measured at $z\sim4$–10 by HST. An even shallower decline in $\rho_{\rm UV}$ is required in the presence of a radio background excess from black holes or as detected by ARCADE 2. While uncertainties are still too large to rule out any of these scenarios, Figure 1 illustrates the potential of future JWST observations in placing independent constraints on exotic astrophysics during the epoch of the first light.

3. The UV Luminosity Function at Redshift 16

It may be useful at this stage to understand what overall normalization of the galaxy UV LF would be required to produce a 21 cm feature at $z = 16$ in the presence of different radio background excesses. Using the minimal coupling constraints of Madau (2018), and fixing the Schechter LF parameters $M_{\rm UV}^{\star} = -19$ and $\alpha = -2.35$ (from fits provided by Harikane et al. 2023a), we derive at $z = 16$ the normalization $\log_{10}\phi^{\star} = -4.671^{+0.240}_{-0.246}$. Repeating the same procedure for the enhanced $\rho_{\rm UV}$ associated with the early black holes (Ewall-Wice et al. 2018) and ARCADE 2 (Feng & Holder 2018) radio excesses, we obtain $\log_{10}\phi^{\star} = -4.194^{+0.243}_{-0.244}$ and $\log_{10}\phi^{\star} = -3.381^{+0.244}_{-0.247}$, respectively. A summary of these constraints is provided in Table 1.

The best-fit LF in the minimal coupling regime, shown as the solid red line in Figure 2, lies below the LF at $z \sim 12$ calculated by Harikane et al. (2023a) from spectroscopically confirmed candidates, as well as the upper limit at $z \sim 16$ (Harikane et al. 2023a). This fit has a higher normalization, however, when compared to an extrapolation to $z \sim 16$ of the Schechter function parameters provided in Harikane et al. (2023a). The boosted LF of the black hole radiation excess scenario at $z \sim 16$ (brown line) has an approximately similar amplitude/slope to the $z \sim 12$ Harikane et al. (2023a) spectroscopically measured LF at the faint end, but declines more rapidly at the bright end (compare $M_{\rm UV}^{\star} = -19$ versus $M_{\rm UV}^{\star} = -20.3$). This fit still lies below the $z \sim 16$ photometric upper limit. The black curve in Figure 2 represents our prediction for LF of the ARCADE 2 radiation excess scenario, which is approximately 1 order of magnitude higher than the measured LF at $z \sim 12$. Since the latter is constructed using only lower limits, such a significantly boosted LF at $z \sim 16$ cannot be entirely ruled out. Future deep JWST surveys are expected to better probe the $z > 12$ Universe (Wilkins et al. 2023) and may provide a definitive test of these predictions.

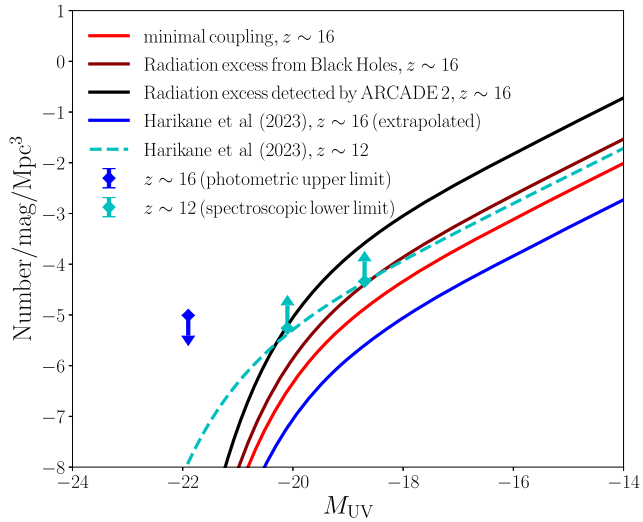

Figure 2. Predicted galaxy UV luminosity function at $z = 16$. The Schechter function parameter $\phi^{\star}$ has been normalized to yield the luminosity density required in the minimal 21 cm coupling (solid red line; Madau 2018), the early black hole radio (brown solid line; Ewall-Wice et al. 2018), and the ARCADE 2 radio excess (black solid line; Feng & Holder 2018) scenarios, at fixed $M_{\rm UV}^{\star} = -21.15$ and $\alpha = -2.35$. The cyan dashed and blue solid curves show the Harikane et al. (2023a) best-fit Schechter function obtained from the spectroscopically confirmed candidates at $z = 9$–12 and extrapolated to $z \sim 16$, respectively. The upper limit (blue arrow) is obtained from photometric estimates at $z \sim 16$, while the lower limits (cyan arrows) represent the spectroscopic constraints by Harikane et al. (2023a). The 21 cm signal constraints predict a much higher number of galaxies than the extrapolation of Harikane et al.'s (2023a) results from $z = 9$ to 12 by approximately 1–3 orders of magnitude at the faint end, depending on the presence and intensity of the radio background.

4. The 21 cm Signal

In the previous section, we have shown how JWST data can constrain the presence of a 21 cm signal at extreme redshifts. Here, we offer a preliminary discussion of the few factors that may influence such feature. We use our default, minimal coupling scenario (see Madau 2018 and Figure 1) for the evolution of the UV luminosity density to compute the expected 21 cm brightness temperature in the absence of X-ray heating and of a radio excess. Figure 3 compares the EDGES-claimed absorption profile to predictions from a canonical model with a cutoff in the UV luminosity density at $z = 20.5$ (dashed red curve) and without such a cutoff (solid red curve). It shows how the absorption trough reported by the EDGES collaboration is several times stronger than that predicted by traditional astrophysical models, and the impact of a cutoff in $\rho_{\rm UV}$ on the onset of the global signal. As mentioned in the Introduction, the SARAS3 (Singh et al. 2022) experiment has contradicted the EDGES detection. In the framework of our minimal coupling scenario, the SARAS nondetection may be explained by the shallower absorption signal predicted by the solid red curve in the figure, where the presence of Lyα sources at redshifts above 20 move the onset of 21 cm absorption to even lower frequencies. Alternatively, X-ray emission from the first generation of astrophysical sources may heat intergalactic gas above the temperature of the CMB, producing at these epochs a faint 21 cm signal in emission. Complications in assessing the impact of early X-ray heating on the detectability of 21 cm absorption include the role of AGNs, the abundance of early X-ray binaries, and the shape of the X-ray SED in the soft band (e.g., Mesinger et al. 2011; Fialkov et al. 2014; Madau & Fragos 2017). We defer a detailed modeling of X-ray heating and radio excess scenarios to a future paper.

5. Conclusion

The epoch of first light provides a unique window to the earliest astrophysical sources of radiation and their impact on the IGM. In this work, we have focused on the possibility that a high star formation efficiency at early times—as implied by early JWST results—may trigger the onset of intense Lyα emission at redshift $z = 16$–18 and produce a cosmic 21 cm absorption signal 200 Myr after the Big Bang. We have shown that a radio signal at the frequencies probed by the EDGES and SARAS experiments may be expected with an extrapolation of the evolving galaxy UV luminosity density measured at $4 \lesssim z \lesssim 12$ by deep HST and JWST observations. If one integrates the UV LF measured by JWST down to $M_{\rm UV} = -13$, then all the observational data suggest a steady mild evolution of $\rho_{\rm UV}(z)$, generating at $z \sim 16$–18 enough Lyα photons to produce a global 21 cm signal via the Wouthuysen–Field effect. A milder evolution of $\rho_{\rm UV}(z)$, as required by exotic models with a radio background excess over the CMB at early epochs may still be consistent with current JWST data given the large uncertainties associated with cosmic variance and the faint-end slope of the galaxy LF. Using a semianalytical model

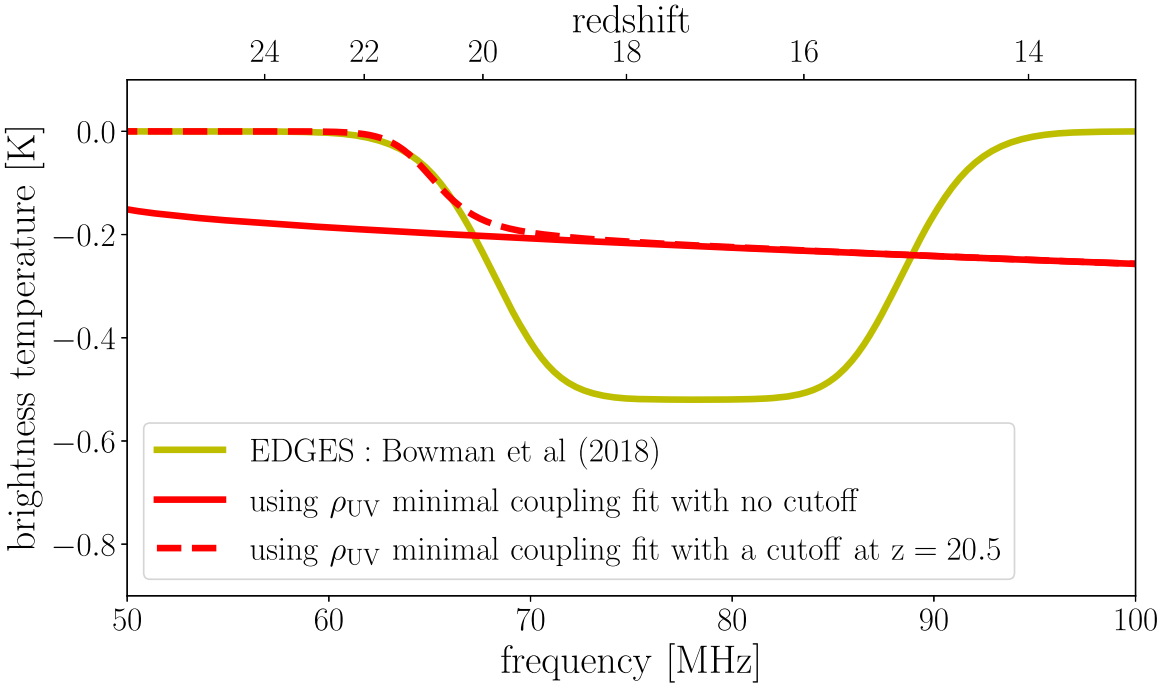

Figure 3. Observed, sky-averaged brightness temperature at 21 cm. The red dashed and solid curves show the prediction from a minimal coupling scenario with a cutoff in the UV luminosity density at $z = 20.5$ and without a cutoff, respectively. The yellow curve shows the spectral feature claimed by the EDGES experiment. The models ignore X-ray heating as well as the possible presence of an excess (over the CMB) radio background.

of reionization, Bera et al. (2022) have recently shown that such a mildly evolving luminosity density requires a much higher contribution from faint galaxies, since massive galaxies at high z are rare.

We note that, using a fixed star formation efficiency linked to the halo mass function predicted by ΛCDM would lead to a significant drop in the UV luminosity density beyond $z > 12$, a decrease that is actually not observed (Sun & Furlanetto 2016; Harikane et al. 2018, 2023a; Mason et al. 2018, 2023). The high UV luminosity density inferred at early times may require a revision of the standard astrophysics of early galaxy formation (Lovell et al. 2023; Mason et al. 2023; Dekel et al. 2023), including the impact of dust (Ferrara et al. 2023; Nath et al. 2023), a top-heavy initial mass function or a high AGN fraction (Inayoshi et al. 2022; Harikane et al. 2023b; Yung et al. 2023), exotic sources such as primordial black holes or Population III stars (Liu & Bromm 2022; Wang et al. 2022; Hütsi et al. 2023; Yuan et al. 2023; Mittal & Kulkarni 2022), or modifications to the cosmological model (Haslbauer et al. 2022; Menci et al. 2022; Maio & Viel 2023; Biagetti et al. 2023; Dayal & Giri 2023; Melia 2023).

During the preparation of this Letter, Meiksin (2023) has independently discussed how the new JWST data may imply the presence of enough Lyα background photons to decouple the spin temperature from that of the CMB by redshift 14. In our work, we have focused on the redshift interval $z \sim 16$–20 where 21 cm experiments like EDGES and SARAS are sensitive.

Acknowledgments

The authors acknowledge the anonymous referee for the constructive feedback and suggestions that greatly improved the paper, and thank Adam Lidz, Martin Rey, Ingyin Zaw, Andrea Macciò, Anthony Pullen, and Patrick Breysse for helpful discussions. S.H. acknowledges support for program number HST-HF2-51507 provided by NASA through a grant from the Space Telescope Science Institute, which is operated by the Association of Universities for Research in Astronomy, incorporated, under NASA contract NAS5-26555. C.C.L. acknowledges support from a Dennis Sciama fellowship funded by the University of Portsmouth for the Institute of Cosmology and Gravitation. P.M. acknowledges support from NASA TCAN grant 80NSSC21K0271 and the hospitality of New York University Abu Dhabi during the completion of this work. This research was supported in part by the National Science Foundation under grant No. NSF PHY-1748958. Part of this work was completed during the KITP GALEVO23 workshop for data-driven astronomy. This material is based upon work supported by Tamkeen under the NYU Abu Dhabi Research Institute grant CASS.

ORCID iDs

Sultan Hassan https://orcid.org/0000-0002-1050-7572
Christopher C. Lovell https://orcid.org/0000-0001-7964-5933
Piero Madau https://orcid.org/0000-0002-6336-3293
Marc Huertas-Company https://orcid.org/0000-0002-1416-8483
Rachel S. Somerville https://orcid.org/0000-0002-6748-6821
Blakesley Burkhart https://orcid.org/0000-0001-5817-5944
Robert Feldmann https://orcid.org/0000-0002-1109-1919
Tjitske K. Starkenburg https://orcid.org/0000-0003-2539-8206
John F. Wu https://orcid.org/0000-0002-5077-881X
Christian Kragh Jespersen https://orcid.org/0000-0002-8896-6496
Joseph D. Gelfand https://orcid.org/0000-0003-4679-1058
Ankita Bera https://orcid.org/0000-0001-7072-570X

References

Adams, N. J., Conselice, C. J., Ferreira, L., et al. 2023, MNRAS, 518, 4755
Arrabal Haro, P., Dickinson, M., Finkelstein, S. L., et al. 2023, Natur, 622, 707
Atek, H., Shuntov, M., Furtak, L. J., et al. 2023, MNRAS, 519, 1201
Barkana, R. 2018, Natur, 555, 71
Bera, A., Hassan, S., Smith, A., et al. 2022, arXiv:2209.14312
Biagetti, M., Franciolini, G., & Riotto, A. 2023, ApJ, 944, 113
Bouwens, R. J., Illingworth, G., Ellis, R. S., Oesch, P., & Stefanon, M. 2022a, ApJ, 940, 55
Bouwens, R. J., Illingworth, G. D., Oesch, P. A., et al. 2015, ApJ, 803, 34
Bouwens, R. J., Stefanon, M., Brammer, G., et al. 2022b, MNRAS, 523, 1036
Bowman, J. D., Rogers, A. E. E., Monsalve, R. A., Mozdzen, T. J., & Mahesh, N. 2018, Natur, 555, 67
Boylan-Kolchin, M. 2023, NatAs, 7, 731
Bradley, L. D., Coe, D., Brammer, G., et al. 2023, ApJ , 955, 13
Bradley, R. F., Tauscher, K., Rapetti, D., & Burns, J. O. 2019, ApJ, 874, 153
Castellano, M., Fontana, A., Treu, T., et al. 2022, ApJL, 938, L15
Castellano, M., Fontana, A., Treu, T., et al. 2023, ApJL, 948, L14
Dayal, P., & Giri, S. K. 2023, arXiv:2303.14239
Dekel, A., Sarkar, K. S., Birnboim, Y., Mandelker, N., & Li, Z. 2023, MNRAS, 523, 3201
Donnan, C. T., McLeod, D. J., Dunlop, J. S., et al. 2023, MNRAS, 518, 6011
Donnan, C. T., McLeod, D. J., McLure, R. J., et al. 2023, MNRAS, 520, 4554
Ewall-Wice, A., Chang, T. C., Lazio, J., et al. 2018, ApJ, 868, 63
Ewall-Wice, A., Chang, T.-C., & Lazio, T. J. W. 2020, MNRAS, 492, 6086
Feng, C., & Holder, G. 2018, ApJL, 858, L17
Ferrara, A., Pallottini, A., & Dayal, P. 2023, MNRAS, 522, 3986
Fialkov, A., & Barkana, R. 2019, MNRAS, 486, 1763
Fialkov, A., Barkana, R., & Visbal, E. 2014, Natur, 506, 197
Finkelstein, S. L., Bagley, M. B., Ferguson, H. C., et al. 2023, ApJL, 946, L13
Finkelstein, S. L., Bagley, M. B., Haro, P. A., et al. 2022, ApJL, 940, L55
Fixsen, D. J., Kogut, A., Levin, S., et al. 2011, ApJ, 734, 5
Fraser, S., Hektor, A., Hütsi, G., et al. 2018, PhLB, 785, 159
Harikane, Y., Inoue, A. K., Mawatari, K., et al. 2022, ApJ, 929, 1
Harikane, Y., Nakajima, K., Ouchi, M., et al. 2023a, arXiv:2304.06658
Harikane, Y., Ouchi, M., Oguri, M., et al. 2023b, ApJS, 265, 5
Harikane, Y., Ouchi, M., Ono, Y., et al. 2018, PASJ, 70, S11
Haslbauer, M., Kroupa, P., Zonoozi, A. H., & Haghi, H. 2022, ApJL, 939, L31
Hills, R., Kulkarni, G., Meerburg, P. D., & Puchwein, E. 2018, Natur, 564, E32
Hütsi, G., Raidal, M., Urrutia, J., Vaskonen, V., & Veermäe, H. 2023, PhRvD, 107, 043502
Inayoshi, K., Harikane, Y., Inoue, A. K., Li, W., & Ho, L. C. 2022, ApJL, 938, L10
Ishigaki, M., Kawamata, R., Ouchi, M., et al. 2018, ApJ, 854, 73
Kannan, R., Springel, V., Hernquist, L., et al. 2023, RNAAS, 524, 2594
Labbe, I., van Dokkum, P., Nelson, E., et al. 2023, Natur, 616, 266
Liu, B., & Bromm, V. 2022, ApJL, 937, L30
Lovell, C. C., Harrison, I., Harikane, Y., Tacchella, S., & Wilkins, S. M. 2023, MNRAS, 518, 2511
Madau, P. 2018, MNRAS, 480, L43
Madau, P., & Fragos, T. 2017, ApJ, 840, 39
Madau, P., Meiksin, A., & Rees, M. J. 1997, ApJ, 475, 429
Maio, U., & Viel, M. 2023, A&A, 672, A71
Mason, C. A., Trenti, M., & Treu, T. 2023, MNRAS, 521, 497
Mason, C. A., Treu, T., Dijkstra, M., et al. 2018, ApJ, 856, 2
McCaffrey, J., Hardin, S., Wise, J., & Regan, J. 2023, arXiv:2304.13755
Meiksin, A. 2023, RNAAS, 2, 71
Melia, F. 2023, MNRAS: Letters, 521, L85
Menci, N., Castellano, M., Santini, P., et al. 2022, ApJL, 938, L5
Mesinger, A., Furlanetto, S., & Cen, R. 2011, MNRAS, 411, 955
Mittal, S., & Kulkarni, G. 2022, MNRAS, 515, 2901
Morishita, T., & Stiavelli, M. 2023, ApJL, 946, L35
Muñoz, J. B., Dvorkin, C., & Loeb, A. 2018, PhRvL, 121, 121301
Naidu, R. P., Oesch, P. A., Setton, D. J., et al. 2022a, arXiv:2208.02794
Naidu, R. P., Oesch, P. A., van Dokkum, P., et al. 2022b, ApJL , 940, L14
Nath, B. B., Vasiliev, E. O., Drozdov, S. A., & Shchekinov, Y. A. 2023, MNRAS, 521, 662
Oesch, P. A., Bouwens, R. J., Illingworth, G. D., Labbé, I., & Stefanon, M. 2018, ApJ, 855, 105
Pérez-González, P. G., Costantin, L., Langeroodi, D., et al. 2023, ApJL, 951, L1
Pospelov, M., Pradler, J., Ruderman, J. T., & Urbano, A. 2018, PhRvL, 121, 031103
Prada, F., Behroozi, P., Ishiyama, T., Klypin, A., & Pérez, E. 2023, arXiv:2304.11911
Robertson, B. E. 2022, ARAA, 60, 121
Sims, P. H., & Pober, J. C. 2020, MNRAS, 492, 22
Singh, S., Jishnu, N. T., Subrahmanyan, R., et al. 2022, NatAs, 6, 607
Singh, S., & Subrahmanyan, R. 2019, ApJ, 880, 26
Slatyer, T. R., & Wu, C.-L. 2018, PhRvD, 98, 023013
Sun, G., & Furlanetto, S. R. 2016, MNRAS, 460, 417
Tozzi, P., Madau, P., Meiksin, A., & Rees, M. J. 2000, ApJ, 528, 597
Wang, X., Cheng, C., Ge, J., et al. 2022, arXiv:2212.04476
Wilkins, S. M., Vijayan, A. P., Lovell, C. C., et al. 2023, MNRAS, 519, 3118
Yan, H., Ma, Z., Ling, C., Cheng, C., & Huang, J.-S. 2023, ApJL, 942, L9
Yuan, G.-W., Lei, L., Wang, Y.-Z., et al. 2023, arXiv:2303.09391
Yung, L. Y. A., Somerville, R. S., Finkelstein, S. L., Wilkins, S. M., & Gardner, J. P. 2023, arXiv:2304.04348
Zavala, J. A., Buat, V., Casey, C. M., et al. 2023, ApJL, 943, L9